

Extremely frequency-widened terahertz wave generation using Cherenkov-type radiation

Koji Suizu¹, Kaoru Koketsu¹, Takayuki Shibuya^{1,2}, Toshihiro Tsutsui¹, Takuya Akiba¹,
and Kodo Kawase^{2,3}

¹ Department of Electrical Engineering, Nagoya University, Furo-cho, Chikusa-ku, Nagoya 464-8603, Japan

² RIKEN, 519-1399 Aramaki-Aoba, Aoba, Sendai 980-0845, Japan

³ EcoTopia Science Institute, Nagoya University Furo-cho, Chikusa-ku, Nagoya 464-8603, Japan
suizu@nuee.nagoya-u.ac.jp

Abstract: Terahertz (THz) wave generation based on nonlinear frequency conversion is promising way for realizing a tunable monochromatic bright THz-wave source. Such a development of efficient and wide tunable THz-wave source depends on discovery of novel brilliant nonlinear crystal. Important factors of a nonlinear crystal for THz-wave generation are, 1. High nonlinearity and 2. Good transparency at THz frequency region. Unfortunately, many nonlinear crystals have strong absorption at THz frequency region. The fact limits efficient and wide tunable THz-wave generation. Here, we show that Cherenkov radiation with waveguide structure is an effective strategy for achieving efficient and extremely wide tunable THz-wave source. We fabricated MgO-doped lithium niobate slab waveguide with 3.8 μm of thickness and demonstrated difference frequency generation of THz-wave generation with Cherenkov phase matching. Extremely frequency-widened THz-wave generation, from 0.1 to 7.2 THz, without no structural dips successfully obtained. The tuning frequency range of waveguided Cherenkov radiation source was extremely widened compare to that of injection seeded-Terahertz Parametric Generator. The tuning range obtained in this work for THz-wave generation using lithium niobate crystal was the widest value in our knowledge. The highest THz-wave energy obtained was about 3.2 pJ, and the energy conversion efficiency was about 10^{-5} %. The method can be easily applied for many conventional nonlinear crystals, results in realizing simple, reasonable, compact, high efficient and ultra broad band THz-wave sources.

©2009 Optical Society of America

OCIS codes: (190.4223) Nonlinear wave mixing; (190.4410). Nonlinear optics, parametric processes

References and links

1. G. D. Boyd, T. J. Bridges, C. K. N. Patel, and E. Buehler, "Phase-matched submillimeter wave generation by difference-frequency mixing in ZnGeP_2 ," *Appl. Phys. Lett.* **21**, 553–555 (1972).
2. A. Rice, Y. Jin, X. F. Ma, X. C. Zhang, D. Bliss, J. Larkin, and M. Alexander, "Terahertz optical rectification from <110> zinc-blende crystals," *Appl. Phys. Lett.* **64**, 1324–1326 (1994).
3. W. Shi, Y. J. Ding, N. Fernelius, and K. Vodopyanov, "Efficient, tunable, and coherent 0.18–5.27-THz source based on GaSe crystal," *Opt. Lett.* **27**, 1454–1456 (2002).
4. T. Tanabe, K. Suto, J. Nishizawa, K. Saito, and T. Kimura, "Tunable terahertz wave generation in the 3- to 7-THz region from GaP," *Appl. Phys. Lett.* **83**, 237–239 (2003).
5. Y. Avetisyan, Y. Sasaki, and H. Ito, "Analysis of THz-wave surface-emitted difference-frequency generation in periodically poled lithium niobate waveguide," *Appl. Phys. B* **73**, 511–514 (2001).
6. D. H. Auston, K. P. Cheung, J. A. Valdmanis, and D. A. Kleinman, "Cherenkov radiation from femtosecond optical pulses in electro-optic media," *Phys. Rev. Lett.* **53**, 1555–1558 (1984).
7. D. A. Kleinman and D. H. Auston, "Theory of electro-optic shock radiation in nonlinear optical media," *IEEE J. Quantum Electron.* **20**, 964–970 (1984).
8. J. Hebling, G. Almási, I. Kozma, and J. Kuhl, "Velocity matching by pulse front tilting for large area THz-pulse generation," *Opt. Express* **10**, 1161–1166 (2002).

9. J. K. Wahlstrand and R. Merlin, "Cherenkov radiation emitted by ultrafast laser pulses and the generation of coherent polaritons," *Phys. Rev. B* **68**, 054301 (2003).
 10. K.-L. Yeh, M. C. Hoffmann, J. Hebling, and K. A. Nelson, "Generation of 10 μ J ultrashort THz pulses by optical rectification," *Appl. Phys. Lett.* **90**, 171121 (2007).
 11. S. B. Bodrov, A. N. Stepanov, M. I. Bakunov, B. V. Shishkin1, I. E. Ilyakov, and R. A. Akhmedzhanov, "Highly efficient optical-to-terahertz conversion in a sandwich structure with LiNbO_3 core," *Opt. Express* **17**, 1871-1879 (2009).
 12. K. Suizu, T. Tutui, T. Shibuya, T. Akiba, and K. Kawase, "Cherenkov phase-matched monochromatic THz-wave generation using difference frequency generation with lithium niobate crystal," *Opt. Express* **16**, 7493-7498 (2008).
 13. T. Shibuya, T. Tsutsui, K. Suizu, T. Akiba, and K. Kawase, "Efficient Cherenkov-Type Phase-Matched Widely Tunable THz-Wave Generation via an Optimized Pump Beam Shape," *Appl. Phys. Express* **2**, 032302 (2009).
 14. D. E. Zelmon, D. L. Small, and D. Jundt, "Infrared corrected Sellmeier coefficients for congruently grown lithium niobate and 5 mol. % magnesium oxide-doped lithium niobate," *J. Opt. Soc. Am. B* **14**, 3319-3322 (1997).
 15. K. Kawase, H. Minamide, K. Imai, J. Shikata, and H. Ito, "Injection-seeded terahertz-wave parametric generator with wide tunability," *Appl. Phys. Lett.* **80**, 195-197 (2002).
 16. Y. Sasaki, H. Yokoyama, and H. Ito, "Surface-emitted continuous-wave terahertz radiation using periodically poled lithium niobate," *Electron. Lett.* **41**, 712-713 (2005).
-

1. Introduction

THz-wave is a very attractive spectral region for advanced applications, such as biomedical analysis and stand-off detection for hazardous materials. The development of monochromatic and tunable coherent THz-wave sources is of great interest for use in these applications. Recently, a parametric process based on second-order nonlinearities was used to generate tunable monochromatic coherent THz-frequency waves using nonlinear optical (NLO) crystals [1-4]. In general, however, nonlinear optical materials have high absorption coefficients in the THz-wave region, which prevents efficient THz-wave generation. High dispersion characteristics between the optical and THz regions in nonlinear optical materials also prevent effective collinear frequency conversion. Quasi-phase matching methods address the phase matching problem, but the tunable range is limited by a nonlinear periodicity in the device. Surface-emitting THz-wave generation efficiently overcomes these problems [5]. Absorption loss is minimized because the THz-frequency wave is generated from the crystal surface. Cherenkov-type radiation is generated as a surface emission [6-11]. This method was adopted for short THz-pulse generation via the optical rectification process. It can be applied in a quasi-continuous wave (typical pulse duration of a few nanoseconds) difference-frequency generation (DFG) process, which can provide monochromatic tunable THz-wave source. We previously demonstrated a Cherenkov phase-matching method for monochromatic THz-wave generation via the DFG process using bulk lithium niobate crystals [12-13]. We were able to generate monochromatic THz radiation with wide tunability, in the range 0.2–4.0 THz. As mentioned in Ref. 13, THz radiation generated far from the crystal surface interfered with that generated near the surface, resulting in destructive interference. Reducing the beam diameter in the propagation direction within the crystal to about one-half the wavelength removed the need to consider phase matching in that direction. However, the tight focusing also reduced the interaction length, decreasing the output power. Here, we demonstrate Cherenkov radiated THz radiation using a MgO-doped lithium niobate slab waveguide, with a thickness of 3.8 μm . The waveguide structure results in a reduction in the beam diameter in the propagation direction, which acts to remove the phase mis-match, and retains a long interaction length.

2. Cherenkov phase matching

The Cherenkov THz-wave is radiated inside the nonlinear crystal when the velocity of the polarization wave excited by the DFG process is greater than the velocity of the radiated wave. Many nonlinear crystals exhibit strong dispersions between the optical and the THz-

wave region. The refractive index at THz frequencies is larger than at optical frequencies, satisfying the Cherenkov-type phase matching condition:

$$\cos \theta_{crystal} = \frac{\lambda_{THz} / n_{THz}}{2L_c} = \frac{\lambda_{THz} / n_{THz}}{\lambda_1 \lambda_2 / (n_1 \lambda_2 - n_2 \lambda_1)} \approx \frac{n_{opt}}{n_{THz}} \quad (1)$$

where λ is a wavelength of the contributing waves in the DFG process ($\omega_1 - \omega_2 = \omega_{THz}$), n_1 , n_2 ($n_1 = n_2 \approx n_{opt}$) and n_{THz} are refractive index of the crystal at pump waves and THz-wave frequencies, respectively, and L_c is the coherence length of the surface-emitted process ($L_c = \pi/\Delta k$, where $\Delta k = k_1 - k_2$ and k is the wave number). The Cherenkov angle, $\theta_{crystal}$, is determined by the refractive indices of the pumping wave and the THz-wave in the crystal, so the angle is strongly dependent on the choice of material. THz-frequency waves radiated at Cherenkov angles propagate to the crystal-air interface, and if the angle is greater than a critical angle (determined by the difference in refractive indices at the interface), the THz-frequency wave is totally reflected at the interface. To prevent total internal reflection, a clad material with a lower refractive index than that of the crystal in the THz range and a proper prism shape, is coupled in at the output.

Figure 1 shows relation of Cherenkov angle and critical angle of several clad materials. We choose polyethylene, diamond, Si and Ge as clad materials, because these materials have low absorbance and low dispersion character at THz frequency region. A total internal reflection occurs below the curve. For example, lithium niobate (LiNbO₃) has 2.2 and 5.2 of refractive index at near infrared and THz-wave region, results in 65 degree of Cherenkov angle in the crystal. On the other hands, critical angle of total internal reflection from the crystal to air, polyethylene, diamond, Si and Ge in a θ manner are 79, 76, 63, 49 and 40 degrees, respectively. The figure tells that diamond, Si and Ge prevent total internal reflection of Cherenkov radiation for lithium niobate crystal.

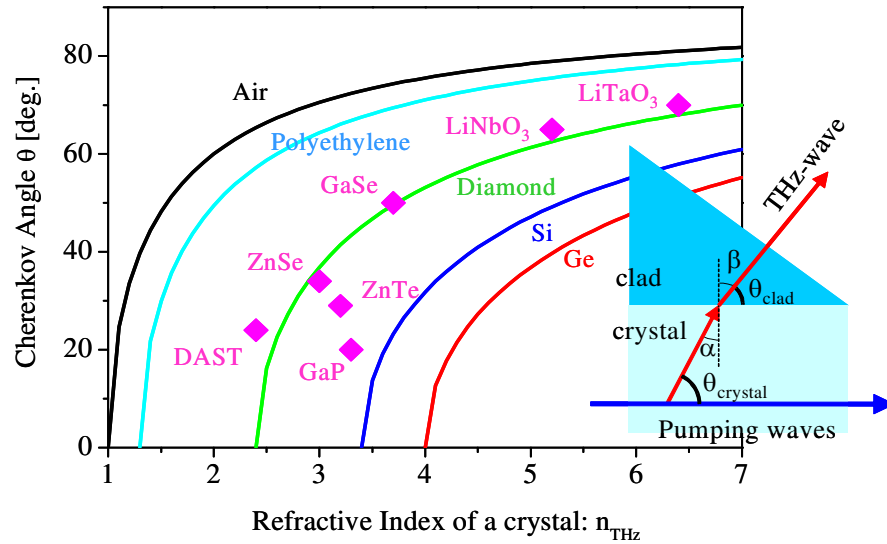


Fig. 1. Cherenkov angle for various nonlinear crystals (pink collared diamonds) and calculated critical angle between a crystal and a clad. Black, aqua, green, blue and red curve represent Air, polyethylene, diamond, Si and Ge as a clad material, respectively. A total internal reflection occurs below the curve. Inset shows a schematic of Cherenkov radiation and output coupling of a THz-frequency wave.

The angle in the clad material, θ_{clad} , is determined by Snell's law (as shown in an inset of Fig. 1), using the refractive index of the clad material n_{clad} .

$$\begin{aligned}\theta_{\text{clad}} &= \frac{\pi}{2} - \beta = \frac{\pi}{2} - \arcsin\left(\frac{n_{\text{THz}}}{n_{\text{clad}}} \sin(\alpha)\right) = \frac{\pi}{2} - \arcsin\left(\frac{n_{\text{THz}}}{n_{\text{clad}}} \sin\left(\frac{\pi}{2} - \theta_{\text{crystal}}\right)\right) \\ &= \frac{\pi}{2} - \arcsin\left(\frac{n_{\text{THz}}}{n_{\text{clad}}} \sin\left(\frac{\pi}{2} - \arccos\left(\frac{n_1 \lambda_2 - n_2 \lambda_1}{n_{\text{THz}}(\lambda_2 - \lambda_1)}\right)\right)\right) \\ &= \arccos\left(\frac{n_1 \lambda_2 - n_2 \lambda_1}{n_{\text{clad}}(\lambda_2 - \lambda_1)}\right)\end{aligned}\quad (2)$$

The radiation angle θ_{clad} , which is important for practical applications, is determined by the refractive indices of the pumping waves in the crystal and the THz-wave in the clad layer. Equation (2) is mathematically equivalent to a model in which the THz-wave is directly radiated to a clad layer. The equation tells us that n_{clad} should be larger than that of the nonlinear crystal in the pumping wave region. A comparison of the refractive indices of various nonlinear crystals with that of Si (about 3.4 in the THz-region) indicates that Si is an appropriate Cherenkov radiation output coupler for many crystals.

In our previous works [12-13], we used 5 mol % MgO-doped lithium niobate and silicon as the nonlinear crystal and clad material, respectively. Although we used bulk lithium niobate crystal, we successfully generated widely-tunable monochromatic THz-frequency waves in the 0.2- to 4.0-THz range. The highest THz-wave energy was about 80 pJ/pulse, and this energy was obtained in a broad spectral region in the 1.0- to 2.0-THz range. Although the generated waves were widely tunable, the THz-wave generation conversion efficiency at higher frequencies (above 2.0 THz) was slightly low. This was caused by a phase mismatch in the generated THz-waves in the direction of propagation, as mentioned in Ref. 13. The pumping wave beam diameters in the lithium niobate crystal in our previous work were 35-127 μm . For a 35- μm pumping beam diameter, the beam width corresponded to about 2.4 cycles of THz waves at 4.0 THz because the refractive index of lithium niobate is about 5.2. THz-frequency waves generated far from the crystal surface interfered with those generated in the neighborhood of the crystal surface, resulting in destructive interference. Reducing the beam diameter width in the crystal in the direction of THz-wave propagation to about one-half the THz wavelength, i.e., about 20 μm , removed the phase mis-matching effect in that direction.

3. Experiments and results

Here, we prepared a slab waveguide of a lithium niobate crystal. A Y-cut 5 mol % MgO-doped lithium niobate crystal on a thick congruent lithium niobate substrate was polished down to 3.8 μm . A thin MgO-doped lithium niobate layer worked as an optical slab waveguide, because the refractive indexes of 5 mol % MgO-doped lithium niobate and congruent lithium niobate at 1300 nm are 2.22 and 2.15, respectively [14]. The waveguide device was 5-mm wide and 70-mm long (X-axis direction). Each X-surface facet was mechanically polished to obtain an optical surface. We demonstrated difference-frequency generation using the experimental setup shown in Fig. 2(b). A dual-wavelength potassium titanium oxide phosphate (KTP) optical parametric oscillator (OPO) with a pulse duration of 15 ns, a pulse energy of 1 mJ and a 1300- to 1600-nm tunable range was used as a pumping source, as in our previous work [12-13]. A thin (3.4- μm thick) polyethylene terephthalate (PET) film was slipped between the array of Si prism couplers and the Y-surface of the MgO-doped lithium niobate crystal. Directly placing an array of Si prism couplers on the Y-surface of the MgO-doped lithium niobate will inhibit the function of the MgO-doped lithium niobate layer as a waveguide for pumping waves, because the refractive index of Si in the near-infrared region is higher (about 3.5) than that of lithium niobate (about 2.2). A PET, in contrast, has a lower refractive index in that region (about 1.3), so adding a thin PET film

does not inhibit the function of the crystal as a waveguide. An array of Si prism couplers on a PET film can work as a coupler for THz-frequency waves, because the PET film is thin compared to the wavelength of a THz-frequency wave. A schematic of the coupling system of the pumping wave and THz-wave emitting system is shown in Fig. 2(a). To couple pumping waves, the pump beam was reduced to few micrometers in the X-axis direction by a 3-mm diameter glass rod lens. The width of the pumping beams in the Z-direction was about 1.9 mm. The waveguide power density was about 53 MW cm^{-2} , estimated from the pump wave pulse energy after waveguide propagation (about $60 \text{ }\mu\text{J}$). We did not observe or calculate the waveguide mode of the structure in which a thin MgO-doped lithium niobate layer was sandwiched by a thick congruent lithium niobate layer and a thin PET film. It remains an area of future work to optimize the waveguide structure. The pump wave and THz-frequency wave polarizations were parallel to the crystal's Z-axis. The THz-wave output was measured with a fixed 4-K Si bolometer.

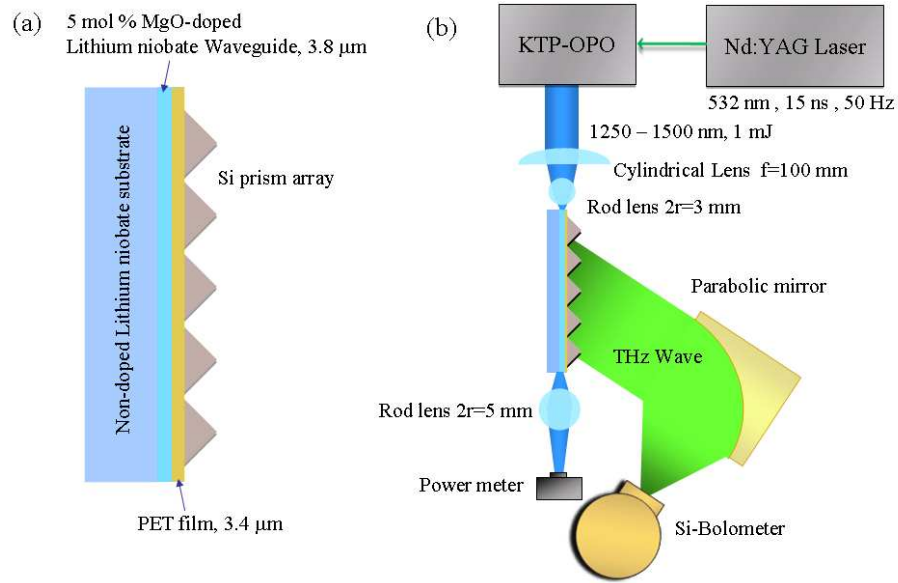


Fig. 2. (a) Schematic of the lithium niobate waveguide device with Si prism array coupler. (b) THz-wave detection experimental setup.

Figure 3 shows a THz-wave spectrum at various wavelength of λ_1 from 1250 to 1400 nm. The spectrum was obtained by varying λ_2 at fixed λ_1 . As shown in Fig. 3, high-frequency THz-wave output ranging to about 7.2 THz was confirmed. We were unable to observe THz-wave generation around 7.2 THz due to very strong THz-wave absorption at 7.5 THz by the LO-phonon mode. The THz-wave spectrum does not depend on pumping wavelength because the near-infrared refractive index is almost constant in the 1250- to 1450-nm range. The inset of the figure 3 shows a comparison of normalized tuning spectrum of the waveguided Cherenkov radiation source and injection seeded terahertz parametric generator (is-TPG) [15]. Nevertheless each THz source were based on a same nonlinear crystal, MgO-doped lithium niobate, a tuning frequency range of waveguided Cherenkov radiation source was extremely widened compare to that of is-TPG. We converted the output voltage of the Si bolometer to the actual THz-wave energy, using the fact that $1 \text{ V} \approx 20 \text{ pJ pulse}^{-1}$ for low repetition rate detection, pulsed heating of the Si device, and an amplifier gain of 1000 at the bolometer. The highest THz-wave energy obtained was about 3.2 pJ, and the energy conversion efficiency from the λ_1 wave ($30 \text{ }\mu\text{J pulse}^{-1}$) was about $10^{-5} \%$. This value is comparable to our previous work on Cherenkov radiation using bulk crystal, despite the low excitation energy of only $30 \text{ }\mu\text{J}$. The tuning range obtained in this work for THz-wave generation using lithium niobate crystal was the widest value in our knowledge.

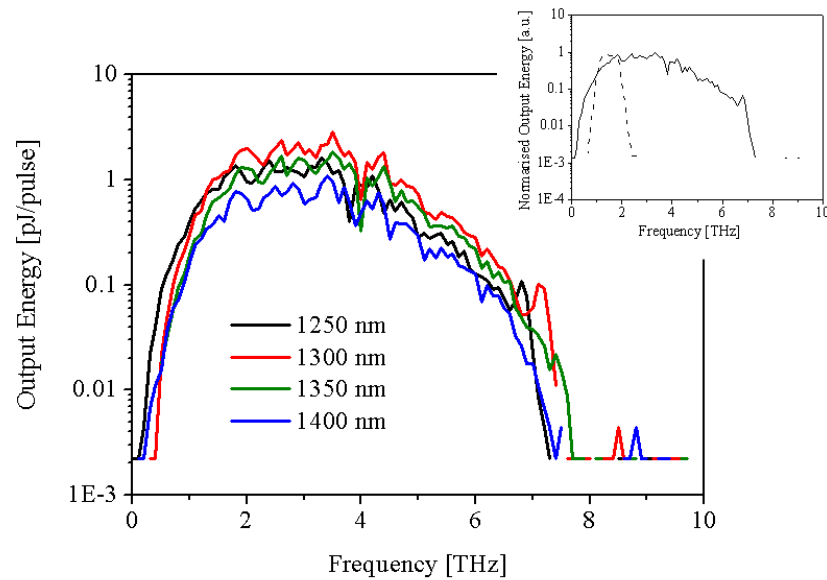


Fig.3 THz-frequency spectrum of waveguided Cherenkov radiation. Black, red, blue and green curves represent 11 pumping wavelengths of 1250, 1300, 1350 and 1400 nm, respectively. An inset 3 shows a comparison of normalized tuning spectrum of the waveguided Cherenkov radiation source under 1250 nm pumping (solid curve) and is-TPG (dashed curve).

The THz-wave emitting angle was absolutely constant, as Si dispersion in this range is almost flat. The device would be work well in an optical rectification process using a femtosecond laser [11]. Such a range, free from structural dips between 0.1 and 7.2 THz, is suitable for ultra-short pulse generation. Also, the surface emission process used here is lossless, permitting the generation of a continuous, widely-tunable THz-frequency range [16], and requiring only two easily commercially available diode lasers. Compact, robust and reasonable THz-wave sources can be realized by this method. Although we demonstrated this method using only a lithium niobate crystal, it can be adopted for other nonlinear crystals, such as LiTaO₃, GaSe, GaP, ZnSe, ZnTe, ZGP, DAST and so on. By choosing the best clad materials for the nonlinear crystals (in many case Si or Ge), the Cherenkov condition is easily satisfied, and control of crystal angles to satisfy phase-matching conditions, such as birefringence phase-matching, is not required. This method opens the door to simple, reasonable, compact, highly efficient and ultra-broadband THz-wave sources.

4. Summary

In conclusion, we successfully widened the tuning range of a monochromatic THz-wave source using Cherenkov radiation based on difference-frequency generation using a lithium niobate waveguide. The range obtained was extremely wide, from 0.1 to 7.2 THz, and exhibited no structural dips in the entire tuning range. This method can be adapted to other nonlinear crystals using simple waveguide fabrication processing techniques.

Acknowledgments

The authors thank Dr. C. Otani and K. Maki of RIKEN, Japan, for their help of using a Si-bolometer.